Thin–Walled Structures 157 (2020) 107109

Contents lists available at ScienceDirect

Thin-Walled Structures

journal homepage: http://www.elsevier.com/locate/tws

Fire performance of cold, warm and hybrid LSF wall panels using numerical studies

Dilini Perera [a], K. Poologanathan [a,*], M. Gillie [a], P. Gatheeshgar [a], P. Sherlock [b], S.M.A. Nanayakkara [c], K.M.C. Konthesingha [d]

[a] Faculty of Engineering and Environment, Northumbria University, Newcastle upon Tyne, UK
[b] ESS Modular, Crag Ave, Clondalkin Industrial Estate, Dublin 22, Ireland
[c] Department of Civil Engineering, University of Moratuwa, Katubedda, Sri Lanka
[d] Department of Civil Engineering, University of Sri Jayawardenepura, Sri Lanka

ARTICLE INFO

Keywords:
Fire performance
Cold-frame
Warm-frame
Hybrid-frame
LSF Wall configurations
Modular walls
Standard fire
FRL

ABSTRACT

Robust and pre-fabrication construction techniques are the cutting edge practice in the building industry. Cold-frame, warm-frame and hybrid-frame are three common Light-gauge Steel Frame (LSF) wall constructions applied for better energy performance. Still, the applications of the aforementioned wall configurations are restricted due to limited fire safety studies. This paper presents the fire performance investigations and results of cold-frame, warm-frame, and hybrid-frame LSF walls together with three novel configurations maintaining the same material quantities. Successfully validated 3D heat transfer finite element models were extended to six wall configurations. Time variant temperature profiles from Finite Element Analyses were evaluated against the established Load Ratio (LR)-Hot-Flange (HF) temperature curve to determine the structural fire resistance. Modified warm-frame construction showed the best performance where the Fire Resistance Level (FRL) is approximately twice that of conventional LSF wall configurations. Hence, the novel LSF wall configurations obtained by shifting the insulation material toward the fireside of the wall make efficient fire-resistant wall solutions and the new designs are proposed to be incorporated in modular constructions for enhanced fire performance.

1. Introduction

Light-gauge Steel Frame (LSF) structures are becoming more common in construction due to their desirable energy and sustainability characteristics. In particular, the use of LSF wall and floor panels is growing in modern low to mid-rise buildings including commercial and residential applications. Depending on the type of construction and the designed load path, load-bearing or non-load bearing types of LSF wall panel configurations are being used in structures [1].

Structural performance, energy performance and fire performance are the major design aspects that need to be addressed [2–7] in LSF wall and floor panel construction. Yet, in the UK and other European countries, while much attention has been given to the energy performance of wall and floor panels, less consideration has been given to the fire performance. In fact, some of the LSF panel designs that have been used in constructions involve combustible insulation material such as expanded polystyrene and polyethylene foam film [6–10]. Meanwhile, researchers like Sayadi et al. [11] Zhou et al. [12] have highlighted the increased risk in case of fire accident when combustible material like Expanded Polystyrene (EPS) insulation is integrated into construction. Fig. 1 depicts two catastrophic failures of LSF panel based structures, which occurred due to accidental fires.

Previous research studies conducted on LSF wall panels have described the effect of thermal insulation, various types of fire-resistant plasterboards, steel sheathing and different stud profiles on fire safety. Dias et al. [13] have experimented on different plasterboard configurations and steel sheathing where internal, external and both internal and external sheathing have resulted in improved fire performance of wall panels. Still, the joints between steel sheathing and plasterboards inherit the risk of being opened up in fire resulting localised buckling failure driving to premature failure in structural criterion which ultimately eliminates the advantage of using steel sheathing.

Moreover, the fire performance of LSF wall panels has been studied with innovative steel studs by Dias et al. [14,15], who showed that a new

* Corresponding author.
E-mail address: keerthan.poologanathan@northumbria.ac.uk (K. Poologanathan).

https://doi.org/10.1016/j.tws.2020.107109
Received 5 May 2020; Received in revised form 20 August 2020; Accepted 2 September 2020
Available online 22 September 2020

Fig. 1. Failures in fire accidents, (a) Lunenglingxiu, Jinan, China; (b): ZIjinyuan, Zhangjia, China [12].

web stiffened channel section performs better when considering ambient and fire conditions. Also, Rusthi et al. [16] experimented with two types of MgO boards in the LSF wall panel, where all three tested wall panels had been failed in the integrity criterion. Soares et al. [10] and McLaggan et al. [17] have studied on the integration of Phase Change Material (PCM) based plasterboards in LSF wall construction which describe the enhanced energy performance but the increase of fire risk and reduction in FRL.

As per the present knowledge and understanding of LSF panel fire performance, integration of cavity insulation between LSF wall studs leads to reduced structural FRL, though it results in increased insulation FRL and energy performance [18]. When the LSF wall has fire on one side, this will result in high temperatures on the fireside and low temperatures on the unexposed side. Hence the load-carrying cold-formed steel studs will be subjected to differential temperature distribution, where the fireside flange is referred to as Hot Flange (HF) and the ambient side flange as Cold Flange (CF). As the temperature difference between HF and CF increases, the difference of stress-strain characteristics between HF and CF is also increased. This will induce thermal bowing of the cold-formed steel studs, which would ultimately lead to increased eccentricity of load applied on studs and to the structural failure [19].

In the case of an insulated LSF wall panel, the thermal insulation acts

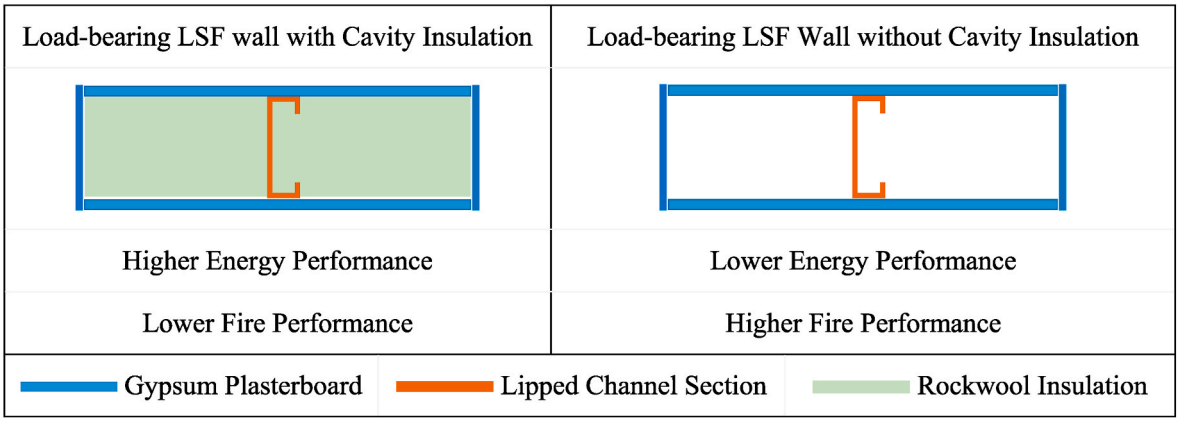

Fig. 2. Features of LSF wall with and without cavity insulation.

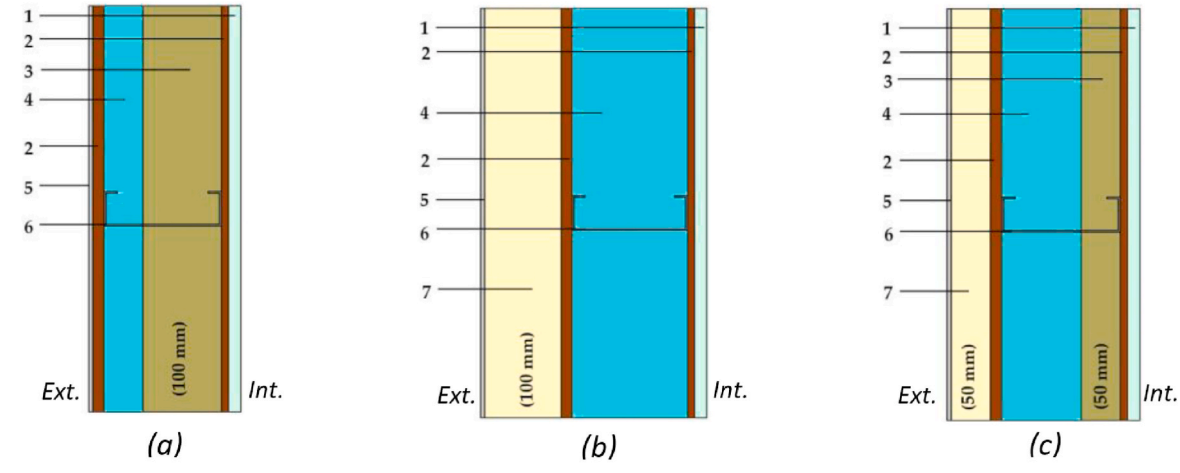

Fig. 3. Wall configurations in current practice, (a): Cold-Frame; (b): Warm-Frame & (c): Hybrid-Frame [6].

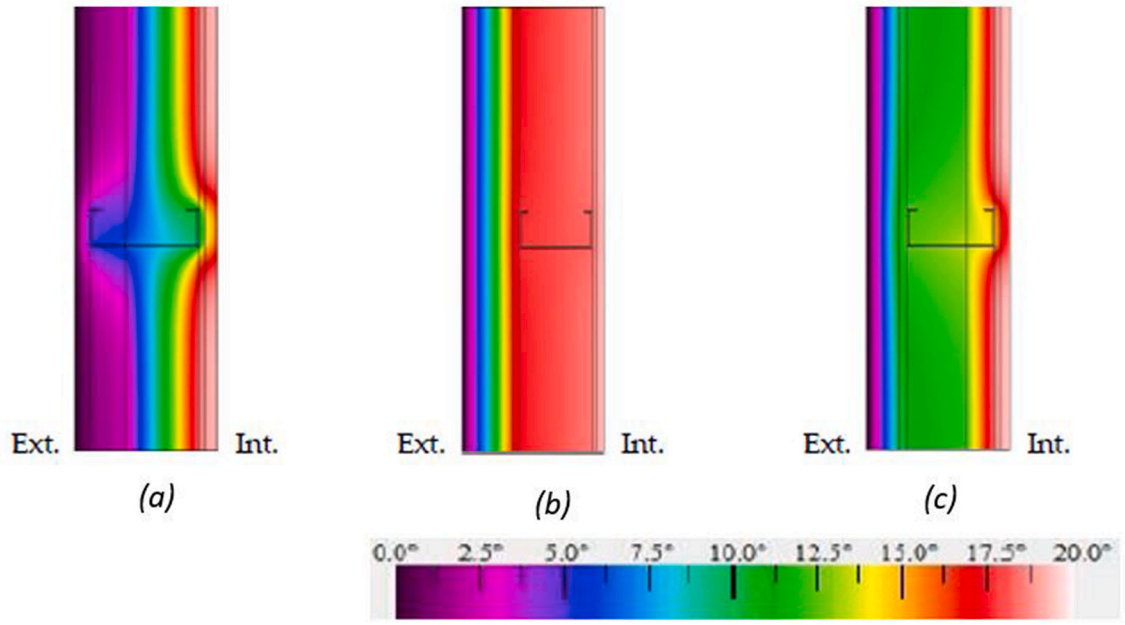

Fig. 4. Temperature distribution of thermal analyses, (a): Cold-Frame; (b): Warm-Frame & (c): Hybrid-Frame [6].

as a barrier to the transfer of heat which will increase the differential temperature between HF and CF to the critical value in a shorter time period. Hence, the FRL of a load-bearing LSF wall is reduced when cavity thermal insulation is applied. Fig. 2 describes the effect of insulation on the fire performance of a load-bearing LSF wall.

As a solution to the reduced structural fire performance related to the integration of cavity insulation, the insulation material can be shifted to the outside of the load-bearing LSF wall. With this improvement both energy and fire performance enhancement could be expected, however, the increased wall thickness might limit the application of this type. Cold-frame, warm-frame and hybrid-frame constructions are some of the extensively used LSF wall constructions of where the location of thermal insulation is changed. Cold-Frame wall construction includes the insulation material inside the wall cavity; where the insulation is shifted in full and partial to the external side of the wall to obtain Warm-Frame and Hybrid-Frame wall constructions respectively. Cold-frame, warm-frame and hybrid-frame LSF wall panel constructions shown in Fig. 3 have been investigated for energy performance by Roque and Santos [6]. Thermal analyses results of these three wall configurations that have been extracted from the study are presented in Fig. 4.

However, limited studies have been conducted on cold-frame, warm-frame and hybrid-frame type LSF wall configurations in-fact no study could be found regarding the fire performance. In this study, instead of expanded polystyrene thermal insulation, rock wool insulation material is proposed due to the highly flammable nature of expanded polystyrene and increased risk related to fire accidents as per Sayadi et al. [11] and Zhou et al. [12]. The presented study investigates the fire performance of the above three conventional LSF wall construction together with three new configurations. 3D Heat transfer FE models were developed in ABAQUS [20] and validated against available test data in the previous study by Gunalan et al. [21]. The validated FE models were extended to examine the heat transfer behaviour of six configurations of LSF walls. In-fact the temperature profiles through wall thickness were generated from FE analyses. Moreover, Load-Ratio (LR)-critical HF Temperature curve was established based on extensive experimental and numerical results. These curves were analysed to predict the Period of Structural Adequacy (PSA) values of LSF wall panels under standard fire. The efficiency of employing the cold-frame, warm-frame, hybrid-frame and other three novel configurations is discussed in detail.

2. Present guidelines and knowledge on fire resistance of LSF wall panels

Standards and guidelines on structural fire design of steel-based structures such as Eurocode 3 [22] and Australian and New Zealand Standard [23]; define three basic criteria; 1) structural 2) integrity and 3) insulation. Structural failure occurs when the component fails to carry the design load when subjected to fire; Integrity failure is defined as the failure to keep transfer of hot gases and flames from fireside to the unexposed side through the structure; The insulation failure is when the temperature on the unexposed surface of the structure exceeds 140 °C on average or 180 °C at any point [16]. The convention of denoting the FRL is Time to (Structural Failure)/(Integrity Failure)/(Insulation Failure). i.e. The FRL of 60 min of a load-bearing LSF Wall panel is denoted as 60/60/60 where the 60 min FRL of a non-load bearing LSF Wall is presented as -/60/60.

The Advanced Calculation Models in Eurocode 3 can be used for the structural fire design of steel structures, however LSF walls considered in the study are composite structures which consist of different types of plasterboard and insulation material in addition to the cold-formed steel studs. Hence, when conducting the structural fire design of LSF panels, a finite element model (FEM) has to be developed for a similar LSF panel which has been tested in a full-scale test applying standard fire. The developed FEM has to be validated and then it can be used to predict the performance and FRL of LSF panels with different parametric values.

ABAQUS CAE [20] is one of the leading advanced computer analysis tools available for finite element structural, mechanical and thermal analyses. Three types of FEA techniques available in ABAQUS software are; thermal FEA, sequentially coupled thermal-structural FEA and fully coupled thermal-mechanical FEA. With the correct use of 3D FEA tools in Abaqus, researchers have been able to predict the FRL of LSF panels with respect to a number of variables [18,24].

Moreover, investigating the experimental and finite element analyses in previous studies [25–28] on load-bearing LSF panels fire performance, a relationship between LR and the HF temperature of the wall studs can be established in case of structural fire failure. In-fact, when a load-bearing LSF wall is subjected to fire, the steel studs experience differential temperatures as explained in previous section. Here the time dependent HF temperature will be the maximum steel temperature at all times. Therefore, when HF temperature reaches to the critical

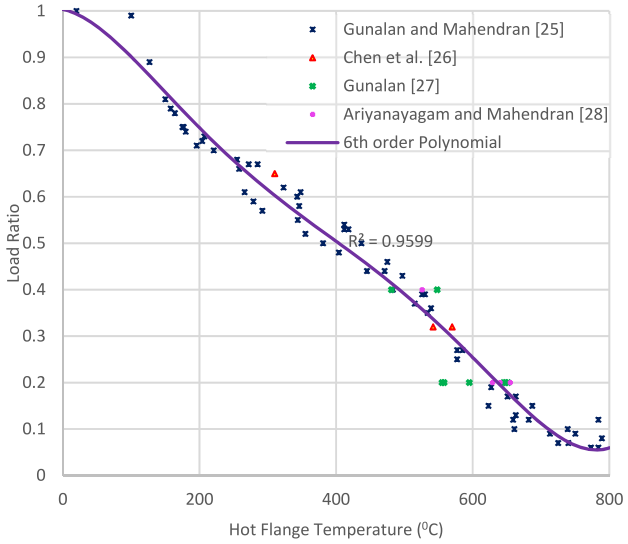

Fig. 5. Load ratio (LR) versus hot flange (HF) Temperature at the structural failure of LSF wall, based on previous studies [25–28].

temperature related to the LR, the steel stud which is in compression will undergo thermal bowing due to the reduced strength at the HF [29,30]. Meanwhile, for LSF floor panels the LR is related to the average temperature of the steel joists which carry the load in bending. Fig. 5 presents the LR versus HF Temperature data at the structural failure of the load-bearing LSF wall studs, which have been extracted from studies by Gunalan and Mahendran, Chen et al. and by Ariyanayagam and Mahendran [25–28]. It should be noted that all experimental tests in Fig. 5 encountered structural failure when standard fire was applied while the numerical test results are also related to the structural FRL.

From this polynomial variation between LR and HF temperature at the structural failure of load-bearing LSF walls, time to structural failure when subjected to standard fire which is the PSA of similar LSF wall panels can be determined once the HF temperature variation is derived from the corresponding thermal FEM.

3. Advanced computer modelling studies

3D Finite Element Heat Transfer models were developed using the commercially available, general-purpose finite element package ABAQUS [20]. The studied six configurations consist of two British Gypsum boards of 15 mm thickness on either side, 150x43x15x2 Lip Channel Sections (LPS) of G500 steel grade and 100 mm thick layer of rockwool insulation.

3.1. LSF wall details

Cold, Warm and Hybrid types of LSF wall frame constructions are some of the commonly practiced LSF walls in the construction industry. The energy performance of these three LSF wall construction options has been studied by Roque and Santos [6]. However, expanded polystyrene has been used for warm and hybrid types that cannot be used in fire-safe constructions as per Sayadi et al. [11] and Zhou et al. [12].

Hence, expanded polystyrene has been replaced with rockwool insulation in this study. Then the cold-frame, warm-frame and hybrid-frame LSF walls and additional three wall configurations (modified warm-frame, partially modified warm-frame and modified cold-frame) using the same amount of material have been numerically investigated, evaluating the FRL for each type based on structural failure. Six wall configurations involved in the study are presented in Fig. 6.

3.2. Elevated temperature thermal properties

When conducting 3D heat transfer finite element analyses, thermal properties of plasterboard material, insulation material and the cold-form steel material are involved and must be specified in a temperature-dependent manner.

Specific Heat, Thermal Conductivity and Density of Steel have been adopted from Eurocode 3 [22]. Similarly, the thermal properties of gypsum boards presented by Rusthi et al. [18] have been extracted. Figs. 7-9 contains the elevated temperature Specific Heat, Thermal Conductivity and Density variation over temperature for Gypsum

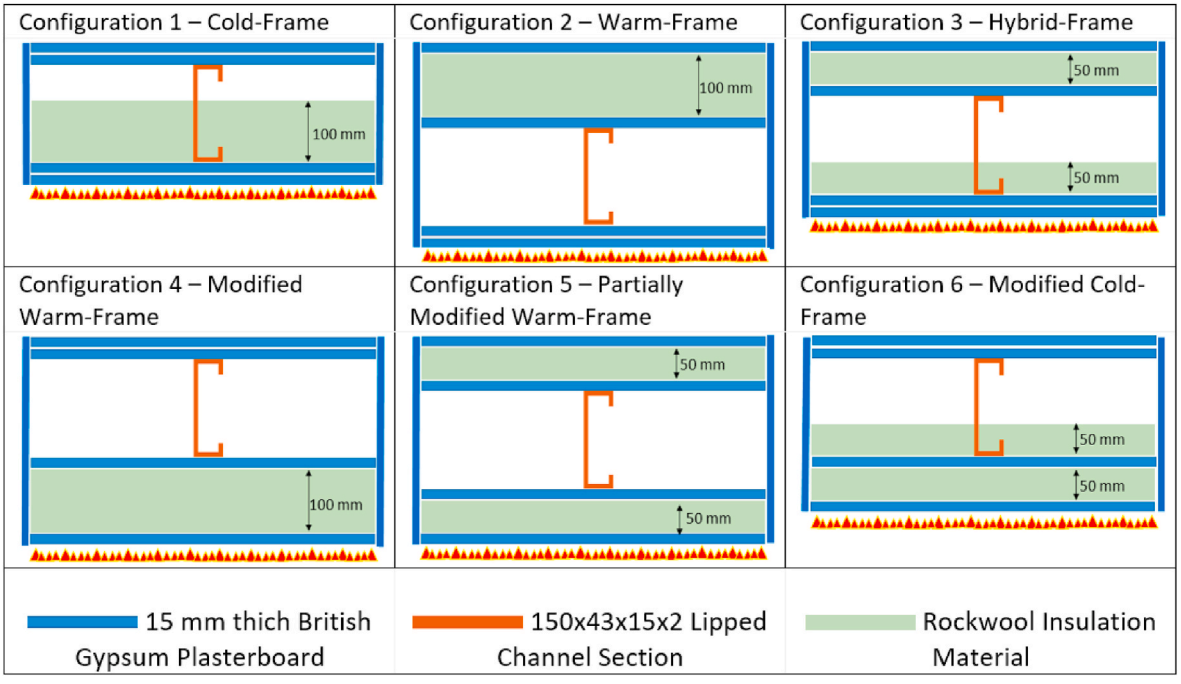

Fig. 6. Investigated load-bearing wall configurations in the study.

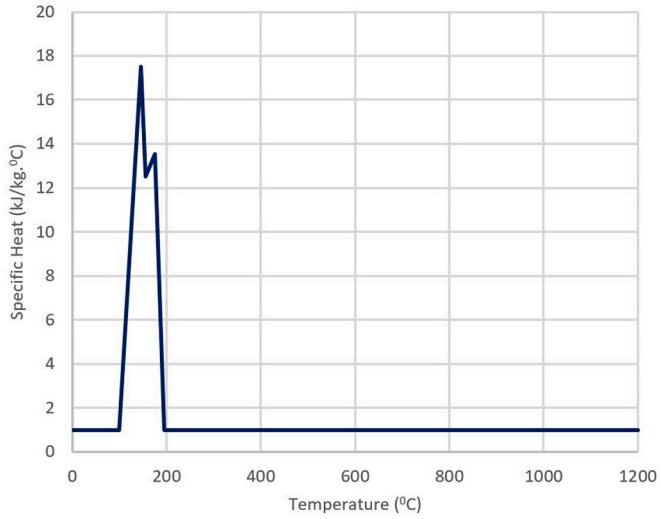

Fig. 7. Specific heat of Gypsum board [18].

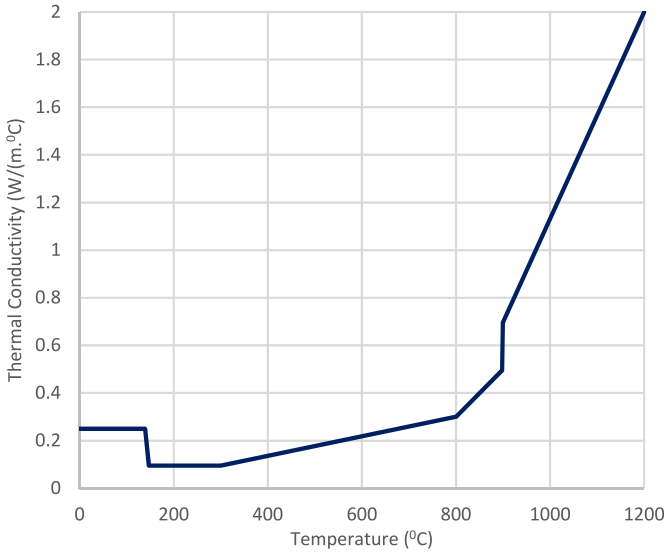

Fig. 8. Thermal conductivity of Gypsum board [18].

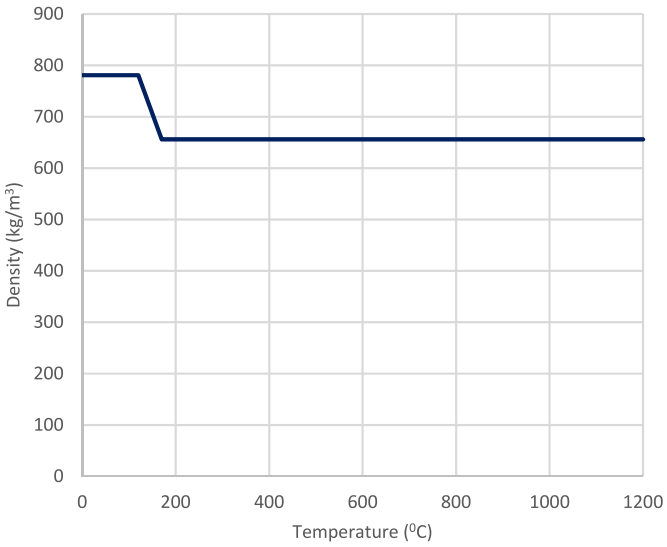

Fig. 9. Density of Gypsum board [18].

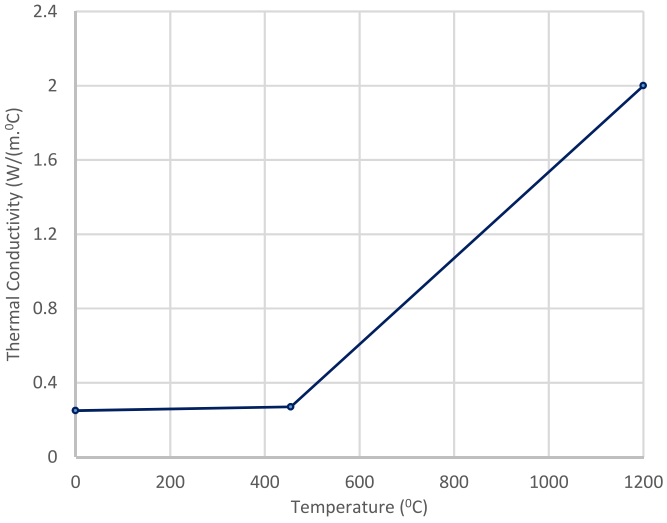

Fig. 10. Thermal conductivity of rockwool insulation [14].

boards. Furthermore, the thermal properties of Rockwool are given in Dias's work [14]. Specific Heat of Rockwool is given as 840 J/(kg.^{0}C), where the density of Rockwool is 100 kg/m^3 [14]. The thermal conductivity of rockwool has a variation over temperature which is shown in Fig. 10.

3.3. Numerical models

FEMs were developed for experimental studies of five LSF wall constructions conducted by Gunalan et al. [21] which have been presented in Table 1. Time-dependent temperature profiles of Fire Side (FS), HF, CF and Ambient Side (AS) of the experimental studies have been compared with the FEA results as shown in Fig. 11.

As per the good agreement between Finite Element and Experimental results, the FEM has been extended to study the fire performance of cold-frame, warm-frame, hybrid frame, modified warm-frame, partially modified warm-frame and the cold-frame constructions. The FEM details are presented in this section.

The LSF walls consist of 3 m long 150x43x15x2 LCS studs at 0.6 m intervals, two Gypsum plasterboards of 15 mm thickness on either side, and a layer of 100 mm thick rockwool insulation. Thermal properties

Table 1
Experimentally tested LSF wall configurations by Gunalan et al. [21].

Model No:	Wall Cross-Section	Insulation	Plasterboard Arrangement	Failure Time (min)
1		None	Single Board	54
2		None	Double Boards	111
3		Glass Fibre	Double Boards	101
4		Rock Fibre	Double Boards	107
5		Cellulose Fibre	Double Boards	110

used for the FEA have been presented in section 3.2. Fig. 12 presents the FEM developed for the cold-frame LSF wall configuration.

All the components of LSF wall configurations were modelled as

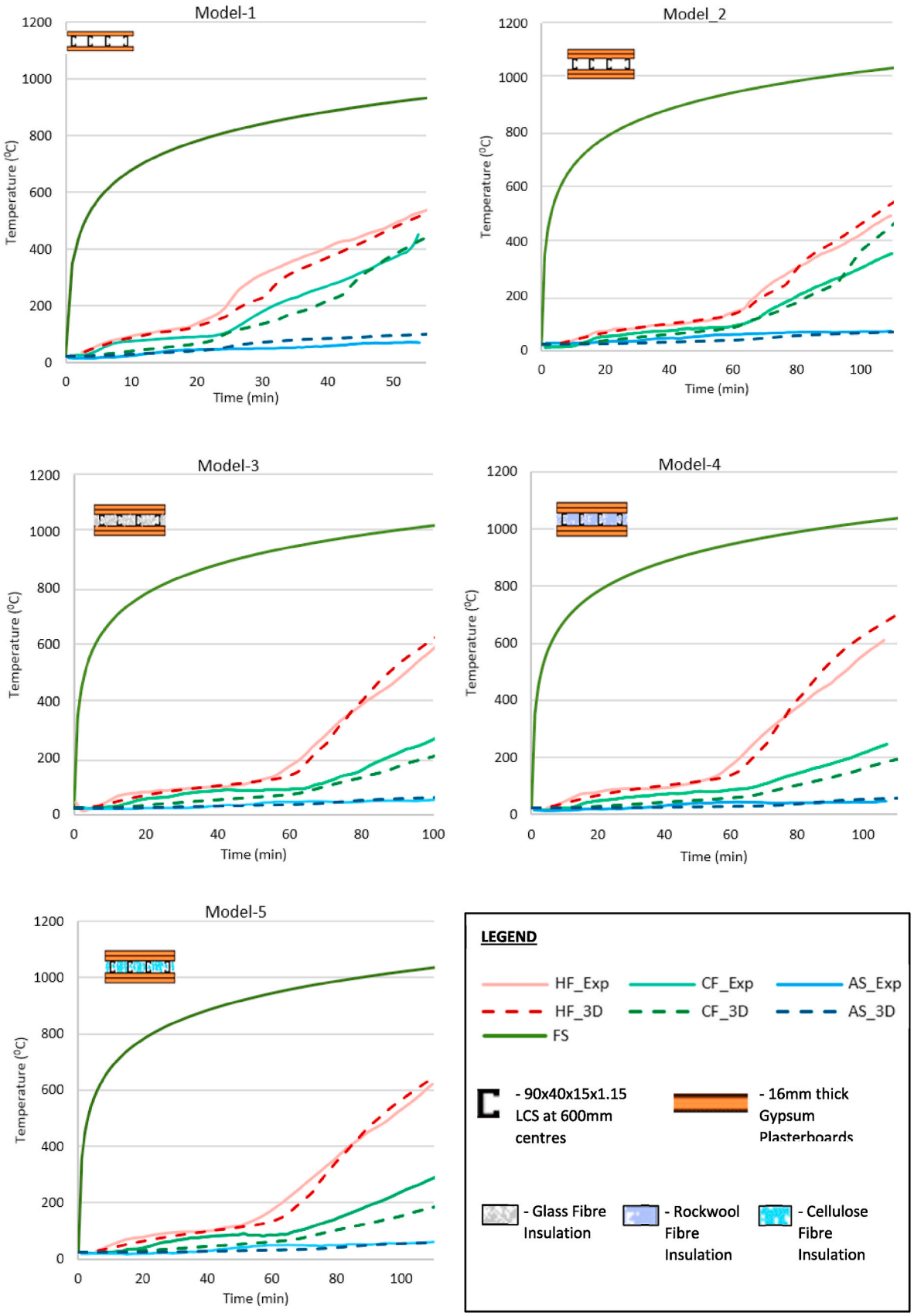

Fig. 11. Experimental [21] and FEA time-temperature variations through wall thickness.

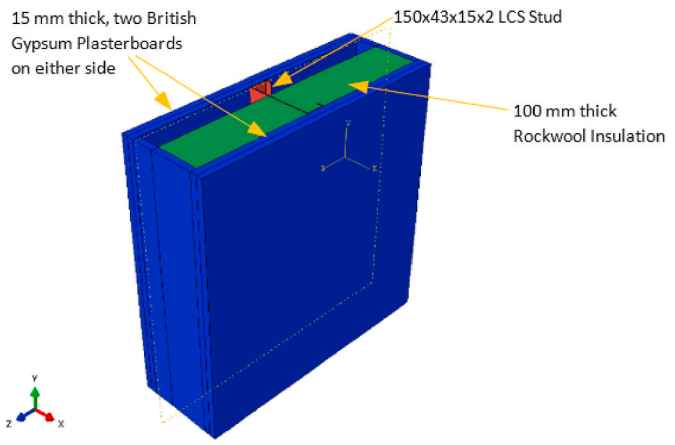

Fig. 12. Developed 3D model of Cold-Frame wall configuration.

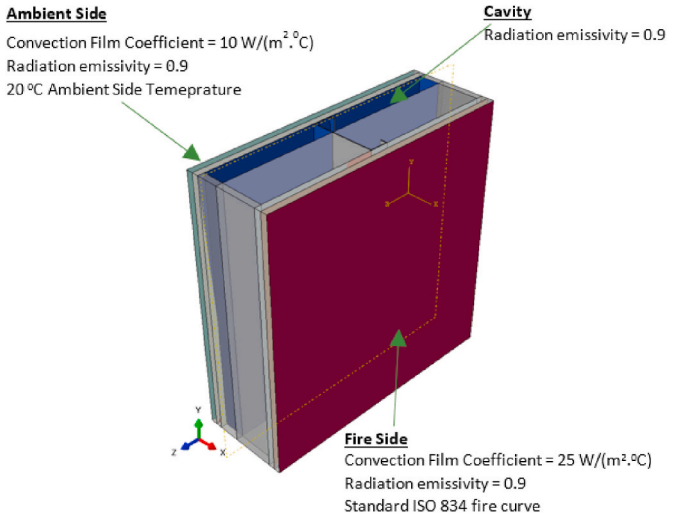

Fig. 13. Boundary conditions applied on the model.

DC3D8 - solid elements and 8-node linear heat transfer brick elements were used to create the mesh. This particular element type ensures conduction mode heat transfer through the elements and from one element to the next in the same material. Global mesh density of 50 mm was applied to the structures while the density through-thickness was set to 2 mm because heat transfer through-thickness is very much significant where as it is negligible in the other two directions. These mesh density details were chosen based on the sensitivity analyses described in Rusthi et al. [18].

As the parts are assembled and positioned, tie constraints were applied between contacting surfaces to enable perfect conduction heat transfer between instances that are in contact.

Two steps have been used for the heat transfer FEA. Initial step was used to apply the ambient temperature to the model while a followed heat transfer step was created as a transient step to apply the standard fire curve and interactions. Initial step size was made 0.1s, where the minimum increment is set to 0.01s with the automatic type steps. Moreover, convection and radiation heat transfer mechanisms were simulated applying appropriate interactions. The convective film coefficients used for fire and ambient sides of the wall were 25 and 10 W/(m^2.^{0}C) respectively while the convection inside the wall cavities was neglected because the airflow inside the wall cavity is restricted. Again the surface radiation was applied on cavity, ambient and firesides of the wall configurations with an emissivity coefficient of 0.9 [31]. The closed cavity method was used for the surface radiation condition of the cavity surfaces [18]. The staged air inside the cavity region could be considered as static and the thermal conductivity of air is comparatively very low. Therefore, convection and conduction mode heat transfer inside the cavity could be reasonably neglected with respect to the heat transfer caused by cavity radiation. The same concept has been practiced in previous research studies [14,18,32] which have been able to accurately simulate the experimental structural fire tests on LSF wall panels.

Standard Fire Curve was applied as temperature boundary conditions on the firesides. Firstly, an amplitude curve was specified following AS 1530.4 for the standard fire curve and then this amplitude was applied for the boundary condition where a heat transfer step function was used. Meanwhile, the room temperature was applied to the whole model as a predefined temperature field in the initial step. The boundary conditions applied on the model are presented in Fig. 13. It should be noted that two plasterboards have been applied at top and bottom of the LSF wall FEMs to simulate the closed cavity condition.

The amplitude curve for the standard fire (ISO 834) was adopted as;

$$\theta = 345log_{10}(8t+1) + 20 \quad (1)$$

which is recommended in AS 1530.4 standard; where θ is the temperature in ^{0}C and t is time in minutes [18]. The ambient temperature of 20 °C has been considered in equation (1).

In Abaqus FEA, the boundary condition of heat flux is calculated based on nodal and sink temperatures. Heat Flux q is expressed as in equation (2) which is applied to all exposed surfaces of the FEM [33].

$$q = h\left(T_{surf} - T_{sink}\right) + \sigma\varepsilon\left(\left(T_{surf} - T_{abs}\right)^4 - \left(T_{sink} - T_{abs}\right)^4\right) \quad (2)$$

where T_{surf} is surface temperature, T_{sink} is the sink temperature, T_{abs} is the absolute temperature, h is the convective heat transfer coefficient, ε is the relative emissivity (0.9) and σ is the Steffan-Boltzmann coefficient $(5.67 \times 10^{-8}\ W/(m^2.^\circ C^4))$.

At the same time, for the heat transfer analyses of cavity volumes, a different model is used. As already described the restrictions applied for convection mode heat transfer inside the cavity, the heat transfer equation used for cavity approximation is based on radiation mode heat transfer as presented in equation (3).

$$q_i^c = \frac{\sigma\varepsilon_i}{A_i}\sum_j \varepsilon_j \sum_k F_{ik}C_{kj}^{-1}\left(\left(T_j - T_{abs}\right)^4 - \left(T_i - T_{abs}\right)^4\right) \quad (3)$$

Where A_i is the area of the ith facet seen to all cavity facets of $j = 1, 2, \ldots, n$; ε_i and ε_j are the relative emissivity of ith and jth facets. k is again a variable from 1,2,..n; F_{ij} and C_{ij} are view factor and reflective matrices while T_i are T_j are the temperatures of ith and jth facets.

3.4. Limitations of finite element studies

Despite the advanced computing tools and options available in the ABAQUS CAE package for FEA, limitations exist such as modelling of plasterboard shrinkage behaviour and initiation of cracks when analysing LSF walls and structures. As Gypsum plasterboards are subjected to fire, the plasterboards lose mass or thin layers of material where the cross-sectional dimensions would reduce. This special behaviour of shrinkage prone material is known as Ablation [31]. Yet, plasterboard thinning effect cannot be modelled using ABAQUS software. Due to loss of mass and plasterboard thinning, heat transfer through plasterboard through conduction will be increased. In the case plasterboard thinning or reduction of material cannot be modelled the measured thermal properties have to be modified to produce correct heat transfer through the plasterboards. Those modified thermal properties which are known as apparent thermal properties of plasterboard and other material have been adopted in the finite element studies as described in section 3.2.

Also when conducting heat transfer analyses, moisture movement through the cavity was not addressed in the FEM due to the complexity of the phenomenon. However, the modified specific heat curves used in

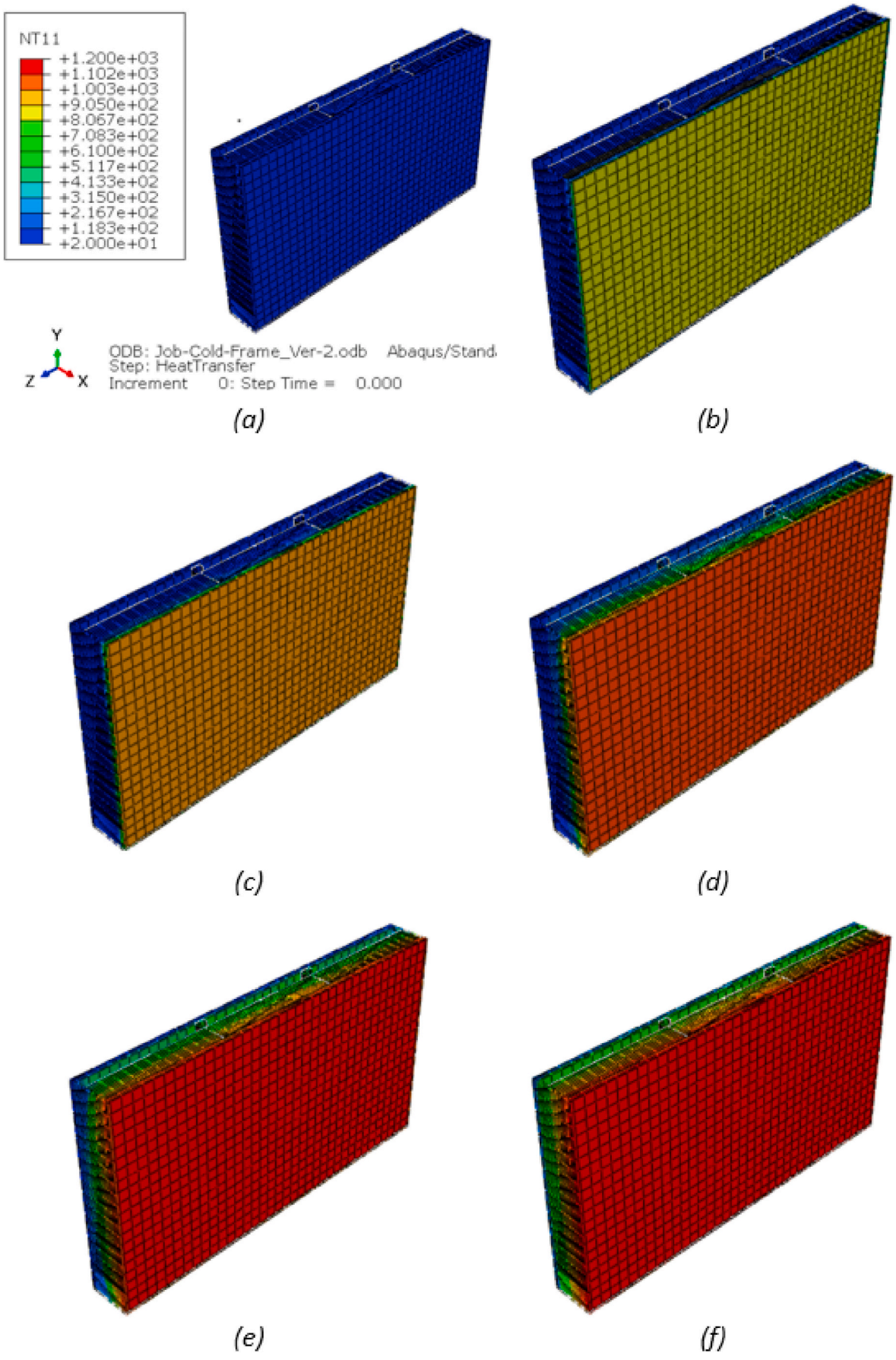

Fig. 14. Nodal temperatures of Cold-Frame wall at different time intervals; (a): 0 min; (b): 30 min; (c): 1h; (d): 2h; (e): 3h; (f): 4h

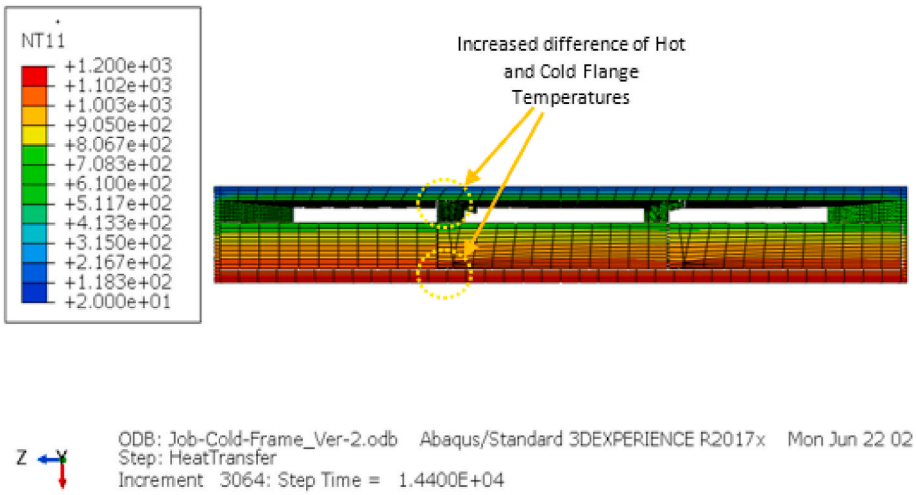

Fig. 15. Plan view of the Cold-Frame model at 4 h.

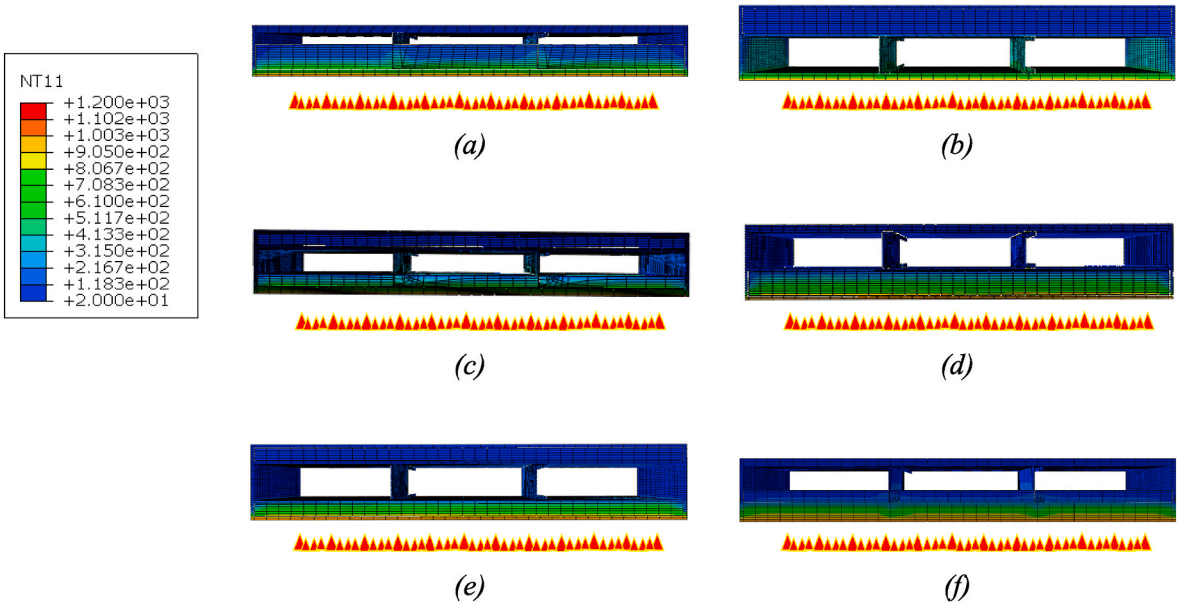

Fig. 16. Plan view temperature contours of (a) Cold-Frame; (b): Warm-Frame; (c) Hybrid-Frame; (d): Modified Warm-Frame; (e): Partially Modified Warm-Frame & (f): Modified Cold-Frame LSF wall panels at 90 min exposure to fire.

the analyses account the effect of moisture content in the material.

Due to the above limitations of the FEM, the study has not addressed the integrity failure criterion for the determination of FRL. Therefore the FRL values have been evaluated for six LSF wall configurations in structural and insulation criteria only.

4. Discussion

3D heat transfer FEM results of six wall configurations have been analysed along with LR versus HF Temperature at the structural failure of LSF wall panels. Fig. 14 demonstrates the temperature distribution of the cold-frame wall model at 0 min, 30 min, 1 h, 2 h and 4 h of exposure to the standard fire ISO 834. A plan view of the model is shown in Fig. 15, in which the temperature difference between the hot and cold flanges of the stud can be identified. Therefore, cavity insulation has increased the risk of thermal bridging effect. This incident can be illustrated more with Fig. 16, which compares the temperature distribution through wall stud at 90 min of fire exposure for all six considered wall configurations. The time dependent temperature profiles for the six wall configurations have been presented in Figs. 18-23 and the temperature values at 90 min exposure to the standard fire have been summarized in Table 2. The maximum temperature difference between HF and CF is seen with cold frame construction which has the whole insulation volume inside the cavity. When half of the cavity insulation is moved to the ambient side and fireside resulting in hybrid-frame and modified cold-frame construction, the temperature deference between HF and CF has been reduced. Moreover, when warm-frame, modified warm-frame and partially modified warm-frame constructions exhibit further reduced temperature difference leading to reduced risk for thermal bridging.

Fig. 5 in section 2 is a presentation of the LR versus critical HF temperature of LSF wall studs for the structural fire failure based on 100 experimental and numerical results. Based on this relationship, the critical temperature of the Hot Flange at 0.6 Load Ratio was found to be 320 °C as presented in Fig. 17. Similarly, Critical Hot Flange Temperature values for 0.4 and 0.8 Load Ratios can be derived from Fig. 17 as presented in Table 3.

From 3D FEA results of the wall configurations when subjected to

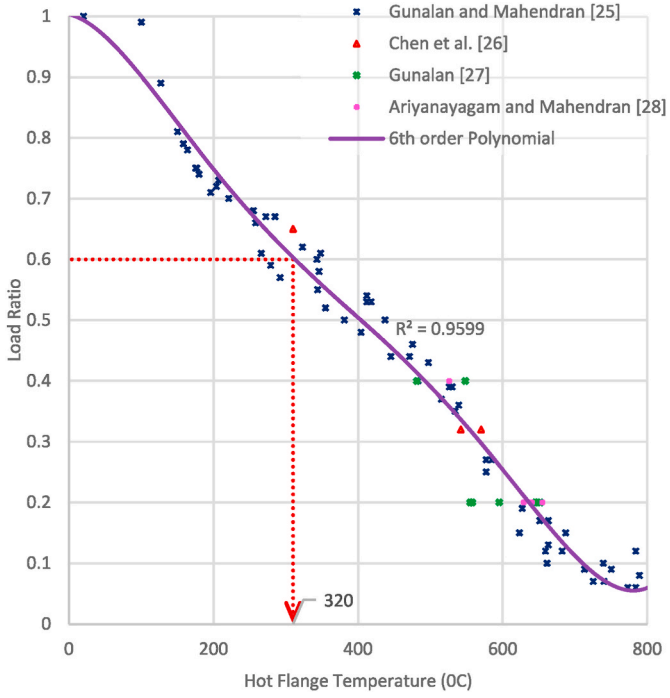

Fig. 17. Critical HF temperature of wall stud at 0.6 LR [25–28].

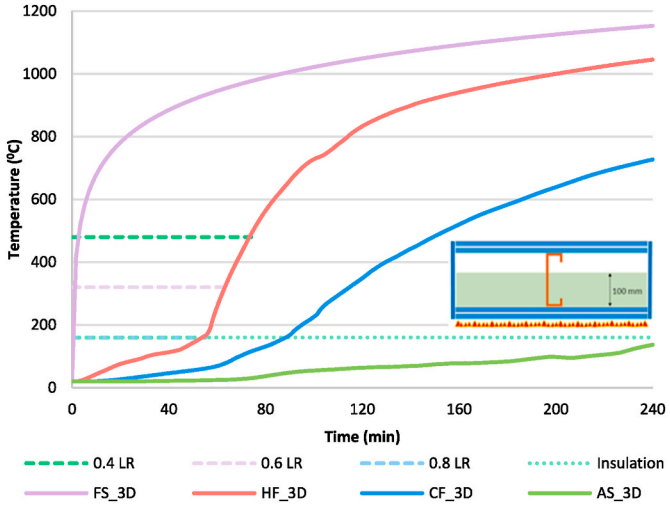

Fig. 18. Cold-Frame 3D Heat Transfer analysis.

standard fire, the temperature variations through wall thickness graphs have been produced. Since the critical hot flange temperature for structural failure at 0.4, 0.6 and 0.8 load ratios has been evaluated, PSA values of structural failure for the Wall configurations can be calculated. Evaluation of PSA of the wall configurations 1 to 6 at 0.4, 0.6 and 0.8 LRs are shown in Figs. 18–23 respectively.

PSA and the FRL values of the 6 wall configurations at 0.4, 0.6 and 0.8 Load Ratios and for NLB scenario, derived from finite element analyses have been summarized in Table 4. When deciding the Structural Fire Resistance, PSA obtained from FEA and LR versus HF Temperature relationship was used. As per AS/NZ: 4600:2018 [23] the FRL is stated in 30 min steps, the same convention has been followed when stating the FRL in this study. Moreover, analyzing the time-dependent temperature variations through wall thickness in FE studies, ambient side maximum temperature for all six wall configurations have remained less than 75 °C at 240 min, which yields that the time to insulation failure to be greater

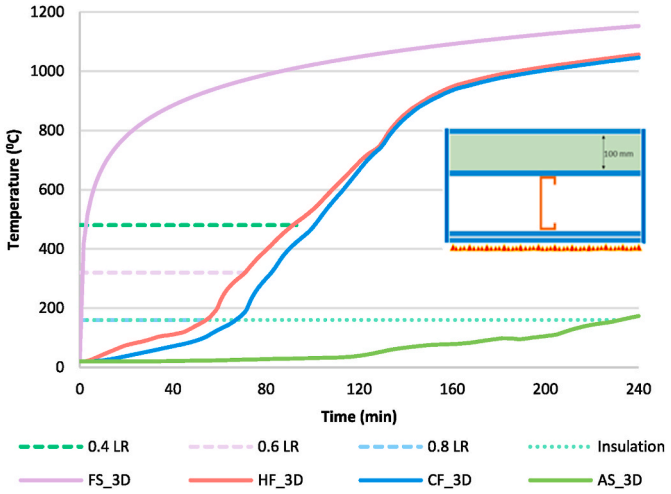

Fig. 19. Warm-Frame 3D Heat Transfer analysis.

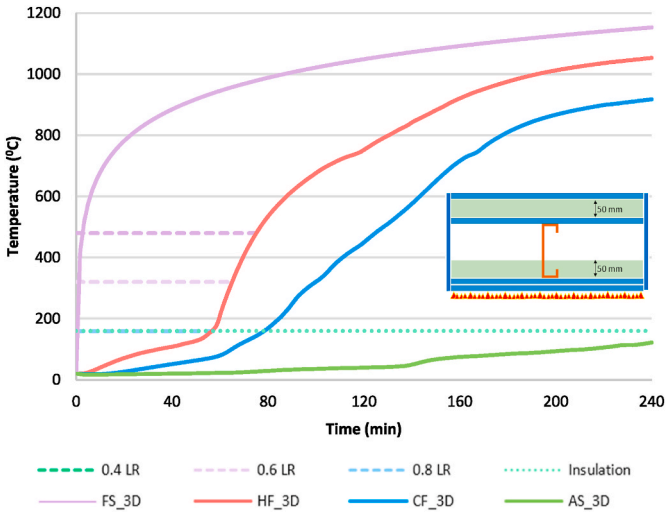

Fig. 20. Hybrid-Frame 3D Heat Transfer analysis.

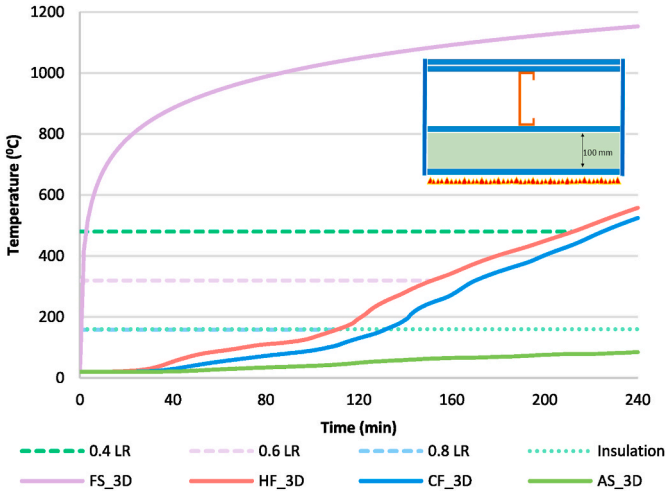

Fig. 21. Modified Warm-Frame 3D Heat Transfer analysis.

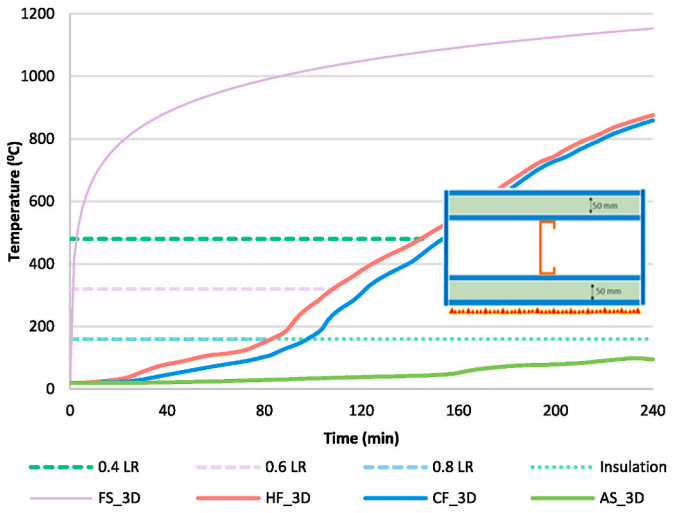

Fig. 22. Partially Modified Warm-Frame 3D Heat Transfer analysis.

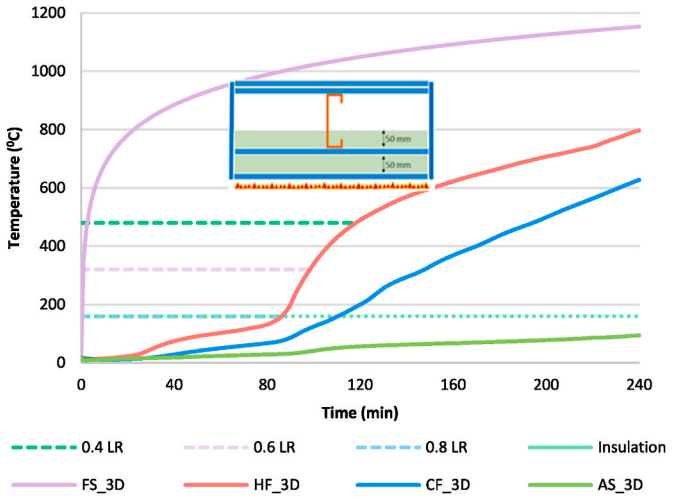

Fig. 23. Modified Cold-Frame 3D Heat Transfer analysis.

than 240 min.

In this study, structural fire failure of load-bearing LSF walls have been investigated where the considered LSF walls consisted of 1–2 mm thick LCS studs. Moreover, all the experiments, FEA and studies were conducted considering standard fire, (ISO 834) on the fireside.

5. Conclusions

The research study is based on the fire performance of six LSF wall constructions which consist of the same amount of building material. Cold-frame, Warm-frame and Hybrid-frame are three LSF wall constructions used in the industry to obtain better energy performance, while a number of previous studies had been conducted on the energy performance of those configurations. However, due to insufficient studies on the fire safety of these wall constructions, this particular numerical study has been conducted on the fire performance of those LSF wall structures and three novel configurations. Moreover, the use of EPS insulation in the conventional warm-frame and hybrid-frame constructions is not acceptable in terms of fire safety so that it has been replaced with rockwool insulation which positively influences both energy and fire performance of the wall. All six construction types; including three existing and three novel configurations, consist of the same amount of material but the position of the insulation has been changed.

Table 2
Temperature differences of LSF wall configurations at 90 min exposure to standard fire, ISO 834.

Wall Specimen	Temperature at 90 min exposure to Standard Fire, ISO 834 (^{0}C)				
	FS	HF	CF	AS	Difference between HF and CF
Cold-Frame	1006	660	168	48	492
Warm-Frame	1006	471	400	30	70
Hybrid-Frame	1006	616	248	33	368
Modified Warm-Frame	1006	118	81	37	37
Partially Modified Warm-Frame	1006	195	133	31	62
Modified Cold-Frame	1006	200	86	31	114

Table 3
Critical HF temperature versus LR.

Load Ratio	0.4	0.6	0.8
Critical Hot Flange Temperature (^{0}C)	490	320	165

Initially, a 3D FEM was developed for an existing experimental study and the results of heat transfer analyses were validated against the experimental results. Subsequently, the validated FEM was extended to assess the behaviour of six wall configurations exposed to standard fire in terms of structural and insulation criterions. Time-dependent temperature profiles derived from heat transfer analyses were analysed against the LR versus HF temperature at the structural failure relationship that was established based on previous experimental and numerical studies in order to evaluate the structural fire resistance of six wall configurations at 0.4, 0.6, 0.8 LRs. At the same time, time-dependent temperature profiles of ambient side of the LSF walls were analysed to determine the insulation fire resistance for each wall configuration.

Modified warm-frame construction exhibits the maximum FRL irrespective of the applied LR. In-fact, the FRL values at 0.6 LR for cold-frame, warm-frame and hybrid-frame LSF walls are in the range of 60 min while that of the modified warm-frame is 150 min, which implies approximately 150% better performance than original wall frame constructions. It is concluded that shifting the whole volume of rockwool insulation to the fireside of the wall as in modified warm-frame configuration leads to enhanced structural fire resistance. Similarly, partial movement of rockwool insulation from ambient side to fireside and from cavity side to fireside creating partially modified warm-frame

Table 4
Period of Structural Adequacy (PSA) of wall configurations.

Configuration	PSA (minutes) at Load Ratios			FRL (minutes)			
				Non-Load-Bearing Walls (NLB)	Load Bearing Walls at Load Ratios		
	0.4	0.6	0.8		0.4	0.6	0.8
Cold-Frame 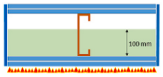	74	63	55	−/−/>240	60/-/>240	60/-/>240	30/-/>240
Warm-Frame 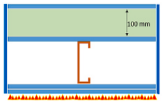	93	72	54	−/−/230	90/-/230	60/-/230	60/-/230
Hybrid-Frame 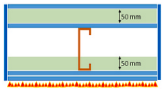	75	65	57	−/−/>240	60/-/>240	60/-/>240	30/-/>240
Modified Warm-Frame 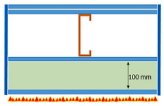	212	150	110	−/−/>240	210/-/>240	150/-/>240	90/-/>240
Partially Modified Warm-Frame 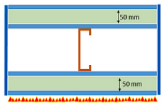	145	110	82	−/−/>240	120/-/>240	90/-/>240	60/-/>240
Modified Cold-Frame 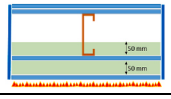	117	98	86	−/−/>240	90/-/>240	90/-/>240	60/-/>240

Notes.
1) Load Ratio (LR) is referred to as the ratio of applied load on a structural element with respect to the load-carrying capacity at the ambient temperature
2) Period of Structural Adequacy (PSA) is the Fire Resistance Level in structural criterion

and modified cold-frame have resulted in increased FRL with respect to the original wall configurations. Therefore, the novel LSF wall configurations are proposed to be incorporated in LSF and modular construction to enhance the fire performance of the structures.

Since the original warm-frame construction had shown the best energy performance due to the elimination of thermal bridging effect, similar behavior should be related to the modified warm-frame construction as well, because the cavity insulation and thermal bridging are eliminated here. However, further research is underway to enhance the understanding and knowledge in this research scope.

Author statement

Authors have participated in concept development, design, analysis and writing.

Declaration of competing interest

The authors declare that they have no known competing financial interests or personal relationships that could have appeared to influence the work reported in this paper.

Acknowledgement

The authors would like to acknowledge the ESS Modular Limited. and Northumbria University for the financial support and research facilities.

References

[1] R.M. Lawson, Light steel modular construction, in: Technical Information Sheet ED014, The Steel Construction Institute, 2012.
[2] S. Selvaraj, M. Madhavan, Investigation on sheathing effect and failure modes of gypsum sheathed cold-formed steel wall panels subjected to bending, Structure 17 (2019) 87–101, https://doi.org/10.1016/j.istruc.2018.09.013. (Accessed 1 February 2019).
[3] J.M. Davies, Light gauge steel cassette wall construction — theory and practice, J. Constr. Steel Res. 62 (11) (2006) 1077–1086, https://doi.org/10.1016/j.jcsr.2006.06.028. (Accessed 1 November 2006).
[4] M. Mortazavi, P. Sharafi, K. Kildashti, B. Samali, Prefabricated hybrid steel wall panels for mid-rise construction in seismic regions, J. Build. Eng. 27 (2020) 100942, https://doi.org/10.1016/j.jobe.2019.100942. (Accessed 1 January 2020).
[5] S. Selvaraj, M. Madhavan, Structural behaviour and design of plywood sheathed cold-formed steel wall systems subjected to out of plane loading, J. Constr. Steel Res. 166 (2020) 105888, https://doi.org/10.1016/j.jcsr.2019.105888. (Accessed 1 March 2020).
[6] E. Roque, P. Santos, The effectiveness of thermal insulation in lightweight steel-framed walls with respect to its position, Special Issue Insul. Mater. Resid. Build. 7 (1) (2017) 18, https://doi.org/10.3390/buildings7010013.
[7] P. Santos, C. Martins, L.S.d. Silva, L. Bragancxa, Thermal performance of lightweight steel framed wall: the importance of flanking thermal losses, J. Build. Phys. 38 (1) (2014) 81–98, https://doi.org/10.1177/1744259113499212.
[8] E. Rodrigues, N. Soares, M.S. Fernandes, A.R. Gaspar, Á. Gomes, J.J. Costa, An integrated energy performance-driven generative design methodology to foster modular lightweight steel framed dwellings in hot climates, Energy Sustain. Develop. 44 (2018) 21–36, https://doi.org/10.1016/j.esd.2018.02.006. (Accessed 1 June 2018).
[9] T. Höglund, H. Burstrand, Slotted steel studs to reduce thermal bridges in insulated walls, Thin-Walled Struct. 32 (1) (1998) 81–109, https://doi.org/10.1016/S0263-8231(98)00028-7. (Accessed 1 September 1998).
[10] N. Soares, P. Santos, H. Gervásio, J.J. Costa, L. Simões da Silva, Energy efficiency and thermal performance of lightweight steel-framed (LSF) construction: a review, Renew. Sustain. Energy Rev. 78 (2017) 194–209, https://doi.org/10.1016/j.rser.2017.04.066. (Accessed 1 October 2017).
[11] A.A. Sayadi, J.V. Tapia, T.R. Neitzert, G.C. Clifton, Effects of expanded polystyrene (EPS) particles on fire resistance, thermal conductivity and compressive strength of

foamed concrete, Construct. Build. Mater. 112 (2016) 716–724, https://doi.org/10.1016/j.conbuildmat.2016.02.218. (Accessed 1 June 2016).
[12] L. Zhou, A. Chen, L. Gao, Z. Pei, Effectiveness of vertical barriers in preventing lateral flame spread over exposed EPS insulation wall, Fire Saf. J. 91 (2017) 155–164, https://doi.org/10.1016/j.firesaf.2017.04.013. (Accessed 1 July 2017).
[13] Y. Dias, M. Mahendran, K. Pologanathan, Full-scale fire resistance tests of steel and plasterboard sheathed web-stiffened stud walls, Thin-Walled Struct. 137 (2019) 81–93, https://doi.org/10.1016/j.tws.2018.12.027. (Accessed 1 April 2019).
[14] Y. Dias, P. Keerthan, M. Mahendran, Predicting the fire performance of LSF walls made of web stiffened channel sections, Eng. Struct. 168 (2018) 320–332, https://doi.org/10.1016/j.engstruct.2018.04.072. (Accessed 1 August 2018).
[15] Y. Dias, P. Keerthan, M. Mahendran, Fire performance of steel and plasterboard sheathed non-load bearing LSF walls, Fire Saf. J. 103 (2019) 1–18, https://doi.org/10.1016/j.firesaf.2018.11.005. (Accessed 1 January 2019).
[16] M. Rusthi, A. Ariyanayagam, M. Mahendran, P. Keerthan, Fire tests of Magnesium Oxide board lined light gauge steel frame wall systems, Fire Saf. J. 90 (2017) 15–27, https://doi.org/10.1016/j.firesaf.2017.03.004. (Accessed 1 June 2017).
[17] M.S. McLaggan, R.M. Hadden, M. Gillie, Fire performance of Phase Change material enhanced plasterboard, Fire Technol. 54 (1) (2018) 117–134, https://doi.org/10.1007/s10694-017-0675-x. (Accessed 1 January 2018).
[18] M. Rusthi, P. Keerthan, M. Mahendran, A. Ariyanayagam, Investigating the fire performance of LSF wall systems using finite element analyses, J. Struct. Fire Eng. 8 (4) (2017) 354–376, https://doi.org/10.1108/jsfe-04-2016-0002.
[19] A.S. Usmani, J.M. Rotter, S. Lamont, A.M. Sanad, M. Gillie, Fundamental principles of structural behaviour under thermal effects, Fire Saf. J. 36 (8) (2001) 721–744, https://doi.org/10.1016/S0379-7112(01)00037-6. (Accessed 1 November 2001).
[20] J.C. Nagetgaal, Computer Process for Prescribing Second-Order Tetrahedral Elements during Deformation Simulation in the Design Analysis of Structures, Google Patents, 2004.
[21] S. Gunalan, P. Kolarkar, M. Mahendran, Experimental study of load bearing cold-formed steel wall systems under fire conditions, Thin-Walled Struct. 65 (2013) 72–92, https://doi.org/10.1016/j.tws.2013.01.005. (Accessed 1 April 2013).
[22] Eurocode 3, Design of Steel Structures - Part 1-2: General Rules - Structural Fire Design, T. E. Union, 2005. (Accessed 23 April 2004).
[23] Joint Technical Committee BD-082 (Ed.), *Cold-formed Steel Structures* (Fire Design, Council of Standards Australia and New Zealand Standards, 2018.
[24] E. Steau, P. Keerthan, M. Mahendran, Thermal modelling of LSF floor systems made of lipped channel and hollow flange channel section joists," Copenhagen, Denmark, September 2017, 2017, pp. 13–15 [Online]. Available: https://onlinelibrary.wiley.com/doi/epdf/10.1002/cepa.313.
[25] S. Gunalan, M. Mahendran, Fire performance of cold-formed steel wall panels and prediction of their fire resistance rating, Fire Saf. J. 64 (2014) 61–80, https://doi.org/10.1016/j.firesaf.2013.12.003. (Accessed 1 February 2014).
[26] W. Chen, J. Ye, Y. Bai, X.-L. Zhao, Improved fire resistant performance of load bearing cold-formed steel interior and exterior wall systems, Thin-Walled Struct. 73 (2013) 145–157, https://doi.org/10.1016/j.tws.2013.07.017. (Accessed 1 December 2013).
[27] S. Gunalan, Structural behaviour and design of cold-formed steel wall systems under fire conditions, in: Doctor of Philosophy, School of Urban Development, Faculty of Environment and Engineering, Quinsland University of Technology, 2011.
[28] A.D. Ariyanayagam, M. Mahendran, Fire performance of load bearing LSF wall systems made of low strength steel studs, Thin-Walled Struct. 130 (2018) 487–504, https://doi.org/10.1016/j.tws.2018.05.018. (Accessed 1 September 2018).
[29] A. Ariyanayagam, M. Mahendran, Experimental study of load-bearing cold-formed steel walls exposed to realistic design fires, J. Struct. Fire Eng. 5 (2014) 291–329, https://doi.org/10.1260/2040-2317.5.4.291, 12/01.
[30] A.D. Ariyanayagam, M. Mahendran, Influence of cavity insulation on the fire resistance of light gauge steel framed walls, Construct. Build. Mater. 203 (2019) 687–710, https://doi.org/10.1016/j.conbuildmat.2019.01.076. (Accessed 10 April 2019).
[31] P. Keerthan, M. Mahendran, Numerical studies of gypsum plasterboard panels under standard fire conditions, Fire Saf. J. 53 (2012) 105–119, https://doi.org/10.1016/j.firesaf.2012.06.007. (Accessed 1 October 2012).
[32] P. Keerthan, M. Mahendran, Thermal performance of composite panels under fire conditions using numerical studies: plasterboards, rockwool, Glass Fibre and Cellulose insulations, Fire Technol. 49 (2) (2013) 329–356, https://doi.org/10.1007/s10694-012-0269-6. (Accessed 1 April 2013).
[33] D. Simulia, ABAQUS Analysis User's Manual, 2020. https://classes.engineering.wustl.edu/2009/spring/mase5513/abaqus/docs/v6.6/books/stm/default.htm?startat=ch02s11ath45.html.